RSC Advances

PAPER

View Article Online
View Journal | View Issue

Cite this: *RSC Adv.*, 2023, **13**, 7877

Chlorination of trichlorosilane/chlorodimethylsilane using metal chlorides: experimental and mechanistic investigations

Rui Duan, [a] Wencai Peng, *[a] Jianshu Zhang *[a] and Jinli Zhang [b]

Removal of carbonaceous impurities from trichlorosilane ($SiHCl_3$) reduces the carbon content of solar grade polysilicon produced with the improved Siemens method. The separation of chlorodimethylsilane $(CH_3)_2SiHCl$ from $SiHCl_3$ by distillation remains challenging due to the small difference in their boiling points. Herein, the chlorination of $(CH_3)_2SiHCl/SiHCl_3$ with metal chlorides (WCl_6, $MoCl_5$) were studied. The aim was to convert $(CH_3)_2SiHCl$ into $(CH_3)_2SiCl_2$, increase the relative volatility of $(CH_3)_2SiHCl$ and $SiHCl_3$ and facilitate the distillation. The optimum reaction conditions were 60 °C, 60 min and n(WCl_6 or $MoCl_5$): n($SiHCl_3$ or $(CH_3)_2SiHCl$) = 0.7 at 0.8 MPa. Under these conditions, and when WCl_6 and $MoCl_5$ were used as the chlorine sources, the extents of $(CH_3)_2SiHCl$ conversion were 22.7 and 18.5 times higher than those of $SiHCl_3$, respectively. In addition, a mechanistic study showed that the difference between the reactions of $SiHCl_3$ and $(CH_3)_2SiHCl$ resulted from the different energy barriers for the reactions of the $SiCl_3^{\cdot}$ and $(CH_3)_2SiCl\cdot$ radicals with WCl_x or $MoCl_x$, and the barrier for the $SiCl_3^{\cdot}$ reaction was higher than that for the $(CH_3)_2SiCl\cdot$ reaction.

Received 5th February 2023
Accepted 22nd February 2023

DOI: 10.1039/d3ra00772c

rsc.li/rsc-advances

1. Introduction

Solar energy is a renewable and clean energy that will play an important role in solving the energy crisis.[1–3] Therefore, polysilicon has rapidly developed as a raw material for solar photovoltaic cells. It is important to limit the impurities contained in solar-grade polysilicon to obtain higher photoelectric conversion efficiencies.

The standard for solar-grade polysilicon requires the carbon atom concentration to be less than 5×10^{18} atoms per cm^3.[4] Currently, the main process used in producing polysilicon is the improved Siemens method.[1,5] Since the final polysilicon product is obtained by reacting $SiHCl_3$ with H_2 in a bell jar furnace,[5] carbon impurities in $SiHCl_3$ should be strictly limited. Therefore, the removal of carbonaceous impurities in $SiHCl_3$ is a key step in the improved Siemens method.

The carbonaceous impurities in $SiHCl_3$ were mainly methylchlorosilanes [$(CH_3)_nSiCl_{4-n}$, n = 1–3].[6] Moreover, the boiling points of CH_3SiHCl_2 (41.9 °C) and $(CH_3)_2SiHCl$ (34.7 °C) are close to the boiling point of $SiHCl_3$ (32.0 °C).[7] Azeotropes are easily formed during $SiHCl_3$ purification *via* distillation. Thus, purifying $SiHCl_3$ by distillation is difficult. One possible method is to convert CH_3SiHCl_2 and $(CH_3)_2SiHCl$ into methylchlorosilanes with high boiling points and high chlorine contents by chlorination. This would result in higher relative volatility and make distillation easier.

Typical chlorine sources for the chlorination reactions of CH_3SiHCl_2 are chlorine gas,[8] chlorinated hydrocarbons[6,9] and chlorosilane.[4,10,11] Wan *et al.*[8] proposed photochlorination of CH_3SiHCl_2 with Cl_2 in a continuous microchannel reactor. The results showed that the removal rate of CH_3SiHCl_2 was as high as 99.67% under the optimal reaction conditions. But this method is currently in the laboratory research stage. In addition, Zhang and Huang[9] reported catalytic chlorination of CH_3SiHCl_2 with carbon tetrachloride (CCl_4) over a Pd/Al_2O_3 catalyst. However, the introduction of new carbon impurities cannot be avoided, and the high price of Pd limits its utilization in industry. Additionally, silicon tetrachloride, a byproduct of polysilicon production *via* a modified Siemens process, can also be used as a chlorine source for chlorination of CH_3SiHCl_2.[4] However, silicon powder is easily formed, blocking the pores of the activated carbon catalyst during this process. Therefore, the catalytic performance and stability of the activated carbon catalyst are poor.

Chlorination of $(CH_3)_2SiHCl$ with LiCl as the chloride source and $B(C_6F_5)_3$ as the catalyst was reported to occur in a mixture of ethyl ether and toluene.[12] Obviously, many researchers are studying chlorination reactions of CH_3SiHCl_2. However, the boiling point of $(CH_3)_2SiHCl$ is closer to that of $SiHCl_3$, which makes separation more difficult. Furthermore, $SiHCl_3$ and $(CH_3)_2SiHCl$ may be chlorinated at the same time. Therefore, it

[a]*School of Chemistry and Chemical Engineering, State Key Laboratory Incubation Base for Green Processing of Chemical Engineering, Shihezi University, Shihezi 832003, China. E-mail: pengwencai@shzu.edu.cn; zjschem@163.com; Tel: +86-993-2057277*
[b]*School of Chemical Engineering and Technology, Tianjin University, Tianjin 300072, China*

is important to study the competitive relationship between the $SiHCl_3$ and $(CH_3)_2SiHCl$ during chlorination reactions.

Metal chlorides are also used as catalysts in chlorination reactions. For instance, (a) chlorination of methylphenyldichlorosilane to chlorinated methylphenyldichlorosilanes with gaseous chlorine has been catalysed by $FeCl_3$, $SbCl_5$, $SnCl_4$ and $AlCl_3$;[13] (b) chlorination of 1,3-dithiolanes and 1,3-dithianes with CH_2Cl_2 has been catalysed by WCl_6;[14] and (c) chlorination of allyl groups in terpenic olefins (β-pinene and carvone) with NaClO has been catalysed by $MoCl_5$, $AlCl_3$, $FeCl_3$ and $FeCl_2$.[15,16] Metal chlorides can be used not only as catalysts but also directly as chlorine sources in reactions, such as in the photochemical chlorination of methane mediated by $FeCl_3$.[17] In addition, the boiling points of WCl_6 (346.7 °C) and $MoCl_5$ (268.0 °C) are very high and they are easily removed by distillation.

Therefore, this work will focus on the thermal chlorination reaction of $SiHCl_3$ and $(CH_3)_2SiHCl$ by using WCl_6 and $MoCl_5$ as chlorine donors. The effects of the metal chloride type, molar ratio of reactants, reaction temperature and reaction time were investigated in detail. Finally, a reaction mechanism was proposed and explored in detail with density functional theory calculations.

2. Experiments and calculations

2.1 Materials used

Analytical standard dimethylchlorosilane ($(CH_3)_2SiHCl$, 99.0%) and trichlorosilane ($SiHCl_3$, 99.0%) were purchased from Sigma-Aldrich. Silicon tetrachloride ($SiCl_4$, 99.0%) was kindly supplied by Xinjiang Daqo New Energy Co. Additionally, dichlorodimethylsilane ($(CH_3)_2SiCl_2$, 99.0%), chloromethyldichloromethylsilane ($(CH_2Cl)CH_3SiCl_2$, 99.0%), tungsten hexachloride (WCl_6, 99.5%) and molybdenum pentachloride ($MoCl_5$, 99.6%) were purchased from Adamas.

2.2 Experimental setup

The specific experimental operations were as follows: first, to prepare stock solutions, $SiHCl_3$ or $(CH_3)_2SiHCl$ was dissolved in $SiCl_4$ at a concentration of 0.5 mol L^{-1}. In addition, a given amount of WCl_6 or $MoCl_5$ and 10 mL of stock solution were added to a 36.5 mL batch reactor. WCl_6 and $MoCl_5$ were easily soluble in $SiCl_4$ and formed homogeneous reaction systems, and the molar ratios of reactants [$n(WCl_6/MoCl_5) : n(SiHCl_3/(CH_3)_2SiHCl)$] were 0.3, 0.7 and 1.2. Next, a nitrogen stream was introduced into the reactor three times to replace the air. To maintain a homogeneous reaction system, the N_2 pressure was raised to a higher reaction pressure (0.8 MPa). Then, the reactor was heated in a water bath and cooled with an ice-salt bath (−20 °C) after the reaction. Finally, the reactor was opened after slowly relieving the pressure. The samples were then removed from the reactor and distilled to remove metal impurities.

The mole fraction of the chlorosilane solution was determined with a 9790 Plus gas chromatograph equipped with a thermal conductivity detector (TCD), and H_2 was used as the carrier gas. The gas chromatography (GC) detection conditions were as follows: a 3 m 25% DC-550/Chromo packed column; an injection temperature of 150 °C; and a detector temperature of 150 °C. In addition, a programmed temperature rise was used for the oven temperature, *i.e.*, it was first held at 60 °C for 2.5 min, then raised to 120 °C at a rate of 30 °C min^{-1}, and finally held at 120 °C for 2.5 min. The identities of the products were determined from the retention times of standard samples.

The conversion of $SiHCl_3$ was calculated according to eqn (1), and it was expressed as $X(SiHCl_3)$. The inlet and outlet mole fractions of $SiHCl_3$ were expressed as $x(SiHCl_3)_{in}$ and $x(SiHCl_3)_{out}$, respectively. The formula used for calculation of the $(CH_3)_2SiHCl$ conversion rate was the same as that used for $SiHCl_3$.

$$X(SiHCl_3) = \frac{x(SiHCl_3)_{in} - x(SiHCl_3)_{out}}{x(SiHCl_3)_{in}} \times 100\% \quad (1)$$

To further identify the components in the reaction product, samples were dissolved in deuterated chloroform ($CDCl_3$) and qualitatively analysed with nuclear magnetic resonance (NMR) spectroscopy using a Bruker Avance III [^1H (400 MHz), ^{13}C (101 MHz)].

2.3 Theoretical method

The reactions discussed herein are free radical reactions, including chain initiation reactions, chain propagation reactions, and chain termination reactions. All the calculations were performed with the Gaussian 16 program.[18] The geometric configuration of each stationary point for a reactant, transition state, or product along the reaction pathway was studied with B3LYP calculations by using the def2-TZVP basis set for the metal atoms and the 6-311G++(2d,p) basis set for the remaining atoms. In addition, frequency analyses were performed to ensure that the structure determined for a reactant or product was at a local minimum (all frequencies were positive) or in a transition state (only one negative frequency). The intrinsic reaction coordinates (IRCs) were used to evaluate whether the structures of the transition states were correctly connected to the products and reactants.[19] The energy (E) in the entire reaction process was taken from the Gibbs free energy in the output file, that is, EE + thermal free energy correction ($T = 298.15$ K). The energy barrier (EB), the energy change (ΔE) and the dissociation energy (DE) were calculated with eqn (2), (3), and (4).

$$EB = E(\text{transition state}) - E(\text{reactant}) \quad (2)$$

$$\Delta E = E(\text{product}) - E(\text{reactant}) \quad (3)$$

$$DE = \sum E(\text{free radicals}) - E(\text{molecular}) \quad (4)$$

3. Results and discussion

3.1 Experimental research on chlorination of $SiHCl_3$/$(CH_3)_2SiHCl$ with WCl_6

3.1.1 Effect of reaction temperature. The influence of reaction temperature on the conversion rate for the reaction of WCl_6 and $SiHCl_3/(CH_3)_2SiHCl$ was investigated over the

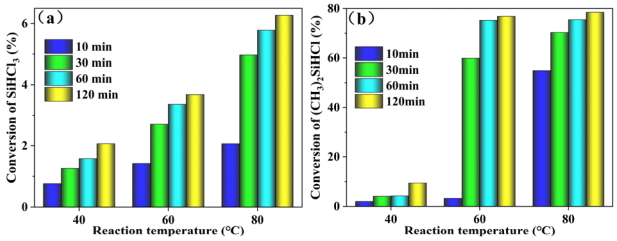

Fig. 1 Conversions of (a) $SiHCl_3$/(b) $(CH_3)_2SiHCl$ in chlorination reactions run with WCl_6 at different reaction temperatures.

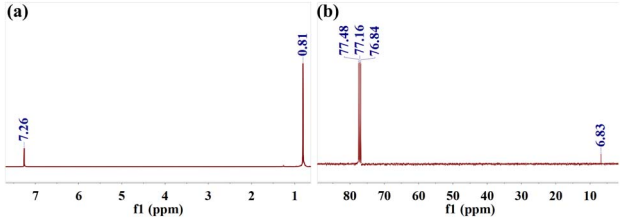

Fig. 3 (a) ^1H NMR and (b) ^{13}C NMR spectra for the product of $(CH_3)_2SiHCl$ chlorination by WCl_6.

temperature range of 40–80 °C with a reaction pressure of 0.8 MPa and $n(WCl_6) : n[SiHCl_3/(CH_3)_2SiHCl] = 0.3$. The $SiHCl_3$ or $(CH_3)_2SiHCl$ conversion rate as a function of temperature is shown in Fig. 1. These results showed that the conversion rates for $(CH_3)_2SiHCl$ and $SiHCl_3$ both increased with increasing temperature and time. The conversion rate of $SiHCl_3$ was extremely low, between 0.8% and 6.3% at 40 °C to 80 °C for 10 min to 120 min. The $(CH_3)_2SiHCl$ conversion was also low, between 2.0% and 9.5%, at 40 °C. However, when the reaction temperature was 60 °C, the conversion of $(CH_3)_2SiHCl$ increased substantially from 3.3% to 59.9% with an increase in the reaction time from 10 min to 30 min. By prolonging the reaction time to 60 min, the conversion of $(CH_3)_2SiHCl$ gradually increased to 75.2%. And the conversion of $(CH_3)_2SiHCl$ increased slightly with increasing temperature and time. Therefore, the optimum reaction conditions were 60 °C for 60 min.

In addition, a solid precipitated from the reaction products obtained with conversion rates greater than 50%. The metal chloride is highly moisture-sensitive, and it was difficult to analyse it further. Since the high-valent tungsten chloride was highly soluble in silicon tetrachloride, $(CH_3)_2SiHCl$ is thought to react with WCl_6 to form a low-valent tungsten chloride or elemental tungsten.

3.1.2 Effect of reactant ratio. The conversions of $SiHCl_3$ or $(CH_3)_2SiHCl$ observed for chlorination reactions run with WCl_6 at different reactant ratios are shown in Fig. 2. Herein, the experimental conditions included a reaction pressure of 0.8 MPa, a reaction temperature of 60 °C and a reaction time of 60 min. When WCl_6 and $(CH_3)_2SiHCl$ were reacted, with increases in the molar ratio of WCl_6 to $(CH_3)_2SiHCl$ from 0.3 to 0.7 and 1.2, the conversion of $(CH_3)_2SiHCl$ increased from 75.2% to 100.0% and 100.0%. The conversion rate of $SiHCl_3$ was far lower than that of $(CH_3)_2SiHCl$. Obviously, the optimum molar ratio of WCl_6 to $(CH_3)_2SiHCl/SiHCl_3$ was 0.7. The ratio of the two conversion rates was 22.7.

The product from the 100% conversion reaction was analysed by GC. It contained a large amount of $(CH_3)_2SiCl_2$ and a small amount of $(CH_2Cl)CH_3SiCl_2$. To further confirm the composition of the sample, the product was qualitatively analysed by ^1H NMR and ^{13}C NMR, as shown in Fig. 3. The main product $(CH_3)_2SiCl_2$ (^1H NMR: 0.81 ppm; ^{13}C NMR: 6.83 ppm) was identified from the NMR spectrum. Therefore, the main product of the reaction between $(CH_3)_2SiHCl$ and WCl_6 was $(CH_3)_2SiCl_2$, and the byproduct was $(CH_2Cl)CH_3SiCl_2$.

3.2 Experimental research on chlorination of $SiHCl_3$/$(CH_3)_2SiHCl$ with $MoCl_5$

3.2.1 Effect of reaction temperature. The conversion rates for $SiHCl_3/(CH_3)_2SiHCl$ in chlorination reactions run with $MoCl_5$ at different temperatures are shown in Fig. 4. Here, the reaction conditions were the same as those used for $SiHCl_3$/$(CH_3)_2SiHCl$ and WCl_6. Similarly, the conversion rates for $(CH_3)_2SiHCl$ and $SiHCl_3$ both increased with increases in temperature and time. The conversion rate of $SiHCl_3$ was very low. $(CH_3)_2SiHCl$ hardly reacted at 40 °C but reacted rapidly at 60 °C and 80 °C. Apparently, the conversion levels for the $MoCl_5$ reaction with $(CH_3)_2SiHCl$ were much higher than those with $SiHCl_3$ at 60 °C and 80 °C. In addition, the conversion of $(CH_3)_2SiHCl$ was as high as 64.0% at 60 °C for 60 min. Therefore, we will continue to explore the effect of the reactant ratio on the conversion of $SiHCl_3/(CH_3)_2SiHCl$ in the chlorination reactions with $MoCl_5$ under these reaction conditions. Additionally, when the products were formed with conversion rates

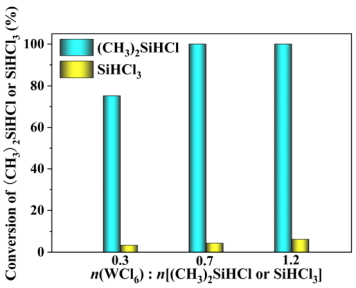

Fig. 2 Conversions of $SiHCl_3/(CH_3)_2SiHCl$ during chlorination of $SiHCl_3/(CH_3)_2SiHCl$ with WCl_6 at different reactant ratios.

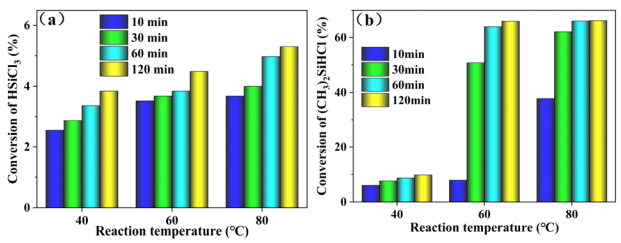

Fig. 4 Conversions of (a) $SiHCl_3$/(b) $(CH_3)_2SiHCl$ in chlorination reactions run with $MoCl_5$ at different reaction temperatures.

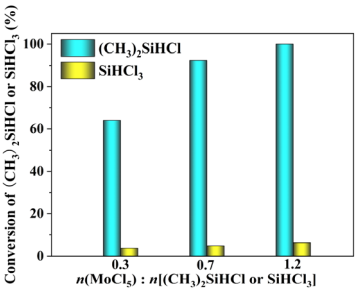

Fig. 5 Conversions of $SiHCl_3$ or $(CH_3)_2SiHCl$ in chlorination reactions run with $MoCl_5$ at different reactant ratios.

greater than 40%, a solid deposit formed during the reaction of $MoCl_5$ with $(CH_3)_2SiHCl$. The reaction was also presumed to yield a low-valent molybdenum chloride or elemental molybdenum.

3.2.2 Effect of reactant ratio. Fig. 5 shows the conversion of $SiHCl_3$/$(CH_3)_2SiHCl$ during chlorination with $MoCl_5$ at different reactant ratios. Herein, the experiment was also carried out at 0.8 MPa, 60 °C and 60 min. Fig. 5 shows that high molar ratios of $MoCl_5$ to $SiHCl_3$/$(CH_3)_2SiHCl$ favoured conversion of $SiHCl_3$ or $(CH_3)_2SiHCl$. As expected, the conversion rate of $(CH_3)_2SiHCl$ was still much higher than that of $SiHCl_3$. When the molar ratio of $MoCl_5$ to $SiHCl_3$/$(CH_3)_2SiHCl$ was 0.7, the ratio of the two conversion levels was the largest at 18.5. Therefore, the optimum conditions were 60 °C, 60 min and $n(MoCl_5) : n(SiHCl_3$ or $(CH_3)_2SiHCl) = 0.7$ for chlorination of $SiHCl_3$/$(CH_3)_2SiHCl$ with $MoCl_5$ at 0.8 MPa. Furthermore, the product formed with 100% conversion was also analysed by GC, ^1H NMR and ^{13}C NMR, which showed that the main product of the reaction between $(CH_3)_2SiHCl$ and $MoCl_5$ was $(CH_3)_2SiCl_2$ and that the byproduct was $(CH_2Cl)CH_3SiCl_2$.

3.3 Mechanism calculation of chlorination of $SiHCl_3$/$(CH_3)_2SiHCl$ with WCl_6

To verify the results of the calculations, the main geometric parameters of $SiHCl_3$, $(CH_3)_2SiHCl$, WCl_6 and $MoCl_5$ were compared with the reported experimental results. It can be seen from the data in Table 1 that the calculated geometric parameters have small errors compared with the experimental values.

Table 1 Calculated and experimental geometric parameters of $SiHCl_3$, $(CH_3)_2SiHCl$, WCl_6 and $MoCl_5$ (bond lengths/Å and bond angles/deg)

		Value	
Compound	Parameter	Calculated	Experimental[20–22]
$SiHCl_3$	Si–H	1.462	1.464
	Si–Cl	2.052	2.020
	Cl–Si–Cl	109.582	109.4
	Cl–Si–H	109.360	109.5
$(CH_3)_2SiHCl$	Cl–Si	2.101	2.0604
	C–Si	1.868	1.8542
	Cl–Si–C	108.37	108.43
	C–Si–C	112.83	112.32
WCl_6	W–Cl	2.316	2.26 ± 0.02
$MoCl_5$	Mo–Cl	2.247[a], 2.324[b]	2.27 ± 0.02

[a] Equatorial plane. [b] Axial direction.

Table 2 Dissociation energies of the W–Cl bonds in WCl_x

Compound	Parameter	DE/kJ mol^{-1}
WCl_6	W–Cl	155.6
WCl_5		202.0
WCl_4		314.2
WCl_3		374.4
WCl_2		389.5
WCl		368.6

3.3.1 Chain initiation reaction. The dissociation energies for the bonds in WCl_x (x indicates the number of chlorine atoms in the metal chloride, and $1 \leq x \leq 6$), $SiHCl_3$ and $(CH_3)_2SiHCl$ are shown in Table 2 and 3. By comparing the dissociation energies, it was found that the bond energy of the W–Cl bonds is the smallest in $SiHCl_3$ and WCl_x ($4 \leq x \leq 6$), with values of 155.6 kJ mol^{-1}, 202.0 kJ mol^{-1} and 314.2 kJ mol^{-1} respectively. Moreover, the Si–H bond, with an energy of 333.3 kJ mol^{-1}, is the weakest bond in $SiHCl_3$, WCl_3, WCl_2, and WCl. Therefore, chain initiation reaction can be divided into cleavage of the Si–H bond and cleavage of the W–Cl bond. Chain initiation involves a decomposition reaction in which Cl· is released from WCl_x (eqn (5)) for the $SiHCl_3$ reaction with WCl_6, WCl_5, and WCl_4. In contrast, in the reactions between $SiHCl_3$ and WCl_3, WCl_2, and WCl, the chain initiation reaction is cleavage of the Si–H bond of $SiHCl_3$ (eqn (6)).

$$WCl_x = WCl_{x-1} + Cl\cdot \quad (5)$$

$$HSiCl_3 = H\cdot + SiCl_3 \quad (6)$$

Correspondingly, in reactions of $(CH_3)_2SiHCl$ with WCl_6, WCl_5 and WCl_4, the chain initiation reaction is cleavage of the W–Cl bond in WCl_x (eqn (5)). In the $(CH_3)_2SiHCl$ reactions with WCl_3, WCl_2 and WCl, the chain initiation reaction involves breakage of the Si–H bond in $(CH_3)_2SiHCl$ (eqn (7)).

$$(CH_3)_2SiHCl = H\cdot + (CH_3)_2SiCl\cdot \quad (7)$$

3.3.2 Chain propagation reaction. In the $SiHCl_3$ reactions with WCl_6, WCl_5 and WCl_4, the chlorine atoms from WCl_x continue to react with $SiHCl_3$. Then, chain growth could occur *via* two reactions: ① in the substitution reaction, Cl· attacks the

Table 3 Dissociation energies for $SiHCl_3$ and $(CH_3)_2SiHCl$

Compound	Parameter	DE/kJ mol^{-1}
$SiHCl_3$	H–Si	333.3
	Si–Cl	379.6
$(CH_3)_2SiHCl$	H–Si	343.5
	H–C	378.4
	Si–Cl	411.9

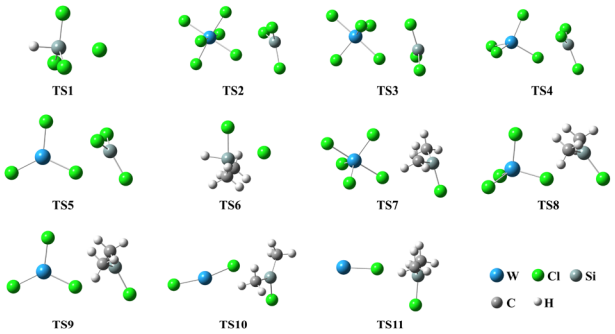

Fig. 6 Structures of transition states formed during the reactions of $SiHCl_3$/$(CH_3)_2SiHCl$ with WCl_6.

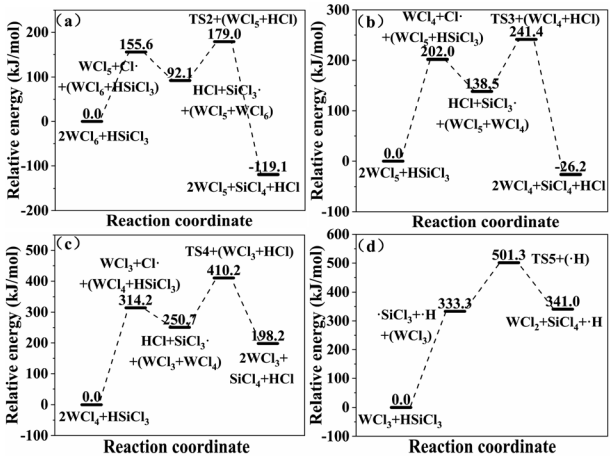

Fig. 7 (a–d) Relative energies for the reactions of $SiHCl_3$ with WCl_x.

silicon atom in $SiHCl_3$ to generate H· and $SiCl_4$, and the energy barrier for this step is 144.8 kJ mol^{-1}. The structure of transition state TS1 involved in this reaction is shown in Fig. 6. ② In the hydrogen abstraction reaction, Cl· abstracts the hydrogen atom on silicon to generate HCl and $SiCl_3$·, and the energy barrier is so small that it can be treated as no energy barrier. DeSain *et al.* also considered the reaction to be a barrierless hydrogen abstraction reaction.[23]

Therefore, when WCl_6, WCl_5 and WCl_4 react with $SiHCl_3$, the chain growth reaction is hydrogen transfer between $SiHCl_3$ and Cl· (eqn (8)). The generated $SiCl_3$· continues to react with WCl_6, WCl_5 and WCl_4 (eqn (9)). In the $SiHCl_3$ reactions with WCl_3, WCl_2, and WCl, $SiCl_3$· from $SiHCl_3$ continues to react with WCl_x (eqn (9)). The relative energies for the reactions of $SiHCl_3$ with WCl_6, WCl_5, WCl_4 and WCl_3 are shown in Fig. 7. The structures of the transition states involved in each reaction are shown in Fig. 6.

$$HSiCl_3 + Cl\cdot = HCl + SiCl_3 \quad (8)$$

$$SiCl_3 + WCl_x = SiCl_4 + WCl_{x-1} \quad (9)$$

In the $(CH_3)_2SiHCl$ reactions with WCl_6, WCl_5 and WCl_4, the Cl· from WCl_x decomposition continues to react with $(CH_3)_2$-SiHCl. There are also two possible chain growth reactions. ① Substitution reaction: Cl· directly attacks the silicon atom in $(CH_3)_2SiHCl$, passes through transition state TS6, and generates H· and $(CH_3)_2SiCl_2$, and the reaction energy barrier is 85.6 kJ mol^{-1}. TS6 is shown in Fig. 6. ② Hydrogen abstraction reaction: Cl· attacks the hydrogen atom on silicon to generate $(CH_3)_2SiCl$· and HCl. This reaction step is also regarded as having no energy barrier.

Therefore, the pathway followed in the reaction of Cl· with $(CH_3)_2SiHCl$ is hydrogen transfer from silicon to the chlorine atom (eqn (10)). The generated $(CH_3)_2SiCl$· continues to react with WCl_6, WCl_5, and WCl_4 to form $(CH_3)_2SiCl_2$ (eqn (11)). In the $(CH_3)_2SiHCl$ reactions with WCl_3, WCl_2, and WCl, $(CH_3)_2SiCl$· and WCl_x react to form $(CH_3)_2SiCl_2$ (eqn (11)). The relative

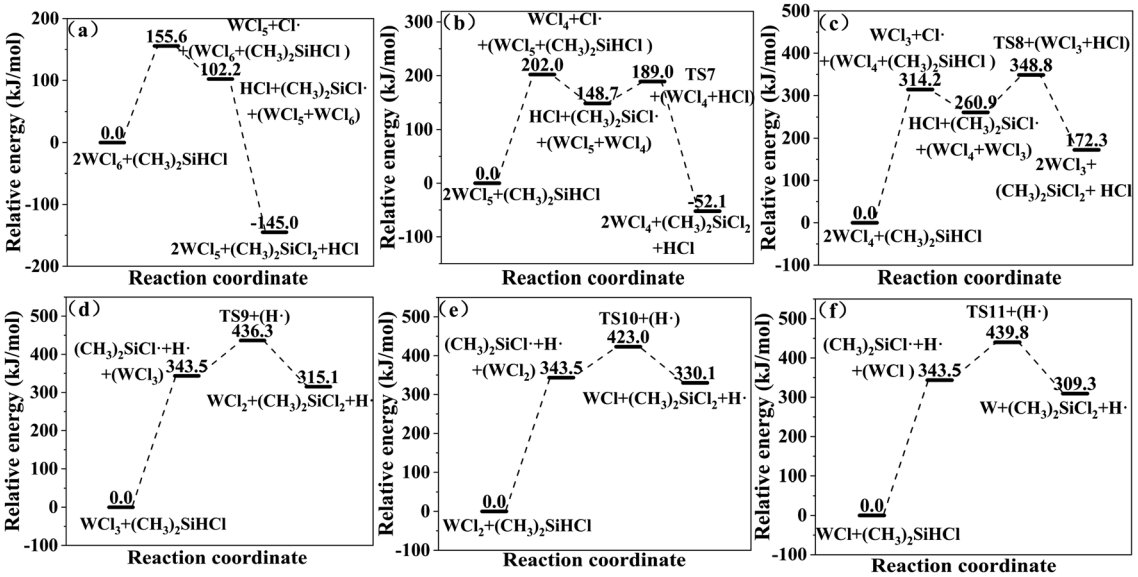

Fig. 8 (a–f) Relative energies for the reactions of $(CH_3)_2SiHCl$ with WCl_x.

Table 4 Energy barriers and Gibbs free energy changes for the reactions of WCl_x with $SiCl_3^{\cdot}$ and $(CH_3)_2SiCl\cdot$

Reactant		EB (kJ mol^{-1})	ΔG^a (kJ mol^{-1})
WCl_6	$\cdot SiCl_3$	86.9	−211.2
	$\cdot(CH_3)_2SiCl$	0	−247.2
WCl_5	$\cdot SiCl_3$	102.9	−164.7
	$\cdot(CH_3)_2SiCl$	40.3	−200.8
WCl_4	$\cdot SiCl_3$	159.5	−52.5
	$\cdot(CH_3)_2SiCl$	87.9	−88.6
WCl_3	$\cdot SiCl_3$	168.0	7.7
	$\cdot(CH_3)_2SiCl$	92.8	−28.4
WCl_2	$\cdot SiCl_3$	—	22.7
	$\cdot(CH_3)_2SiCl$	79.5	−13.4
WCl	$\cdot SiCl_3$	—	1.8
	$\cdot(CH_3)_2SiCl$	96.3	−34.2

[a] The formula used for calculation of ΔG was the same as that for ΔE (eqn (3)).

energies for the $(CH_3)_2SiHCl$ reaction with WCl_6, WCl_5, WCl_4, WCl_3, WCl_2 and WCl are shown in Fig. 8. The structures of the transition states involved in each reaction are shown in Fig. 6.

$$(CH_3)_2SiHCl + Cl\cdot = HCl + (CH_3)_2SiCl\cdot \quad (10)$$

$$WCl_x + (CH_3)_2SiCl\cdot = (CH_3)_2SiCl_2 + WCl_{x-1} \quad (11)$$

Fig. 7 and 8 show that the difference in the reactions of $SiHCl_3$ and $(CH_3)_2SiHCl$ with WCl_x lies in the energy barriers of the $SiCl_3^{\cdot}$ and $(CH_3)_2SiCl\cdot$ reactions with WCl_x. The energy barriers and Gibbs free energy changes of the reactions of WCl_x with $SiCl_3^{\cdot}$ and $(CH_3)_2SiCl\cdot$ are shown in Table 4. The data show that the energy barriers for the reactions of WCl_6, WCl_5, WCl_4 and WCl_3 with $SiCl_3^{\cdot}$ are higher than those for the $(CH_3)_2SiCl\cdot$ reactions, with differences of 86.9 kJ mol^{-1}, 62.6 kJ mol^{-1}, 71.6 kJ mol^{-1} and 75.2 kJ mol^{-1}. These results also show that $\Delta G > 0$ for the reactions of WCl_3, WCl_2, and WCl with $SiCl_3^{\cdot}$ and that $\Delta G < 0$ for the reactions of WCl_3, WCl_2, and WCl with $(CH_3)_2SiCl\cdot$. Obviously, WCl_x reacts more readily with $(CH_3)_2$-SiHCl. These results are consistent with the experimental data, which demonstrates the practicality of the calculations.

3.3.3 Chain termination reaction. At the chain termination stage, free radicals combine with each other to form the bond with the largest bond energy. According to a comparative analysis using the data in Tables 5 and 6, in the reactions of $SiHCl_3$ and $(CH_3)_2SiHCl$ with WCl_6, WCl_5, and WCl_4, chain termination involves reactions of both $SiCl_3^{\cdot}$ and $(CH_3)_2SiCl\cdot$ with $Cl\cdot$ (eqn (12) and (13)). The calculated dissociation energy for H_2 is 436.9 kJ mol^{-1}. Hence, in the reactions of $SiHCl_3$ and $(CH_3)_2SiHCl$ with WCl_3, WCl_2, and WCl, the chain termination reaction involves the combination of two $H\cdot$ (eqn (14)).

$$Cl\cdot + SiCl_3^{\cdot} = SiCl_4 \quad (12)$$

$$(CH_3)_2SiCl\cdot + Cl\cdot = (CH_3)_2SiCl_2 \quad (13)$$

$$2H\cdot = H_2 \quad (14)$$

Table 5 Free radicals and dissociation energies in the chlorination reaction of $SiHCl_3$

DE/kJ mol^{-1}	$\cdot Cl$	$\cdot SiCl_3$
$\cdot Cl$	193.6	366.8
$\cdot SiCl_3$	—	216.4

Table 6 Free radicals and dissociation energies in the chlorination reaction of $(CH_3)_2SiHCl$

DE/kJ mol^{-1}	$\cdot Cl$	$\cdot(CH_3)_2SiCl$	$\cdot CH_2CH_3SiCl_2$
$\cdot Cl$	193.6	402.9	264.0
$\cdot(CH_3)_2SiCl$	—	234.6	275.4
$\cdot CH_2CH_3SiCl_2$	—	—	250.9

In summary, the overall process for $SiHCl_3$ and $(CH_3)_2SiHCl$ reactions with WCl_6, WCl_5 and WCl_4 is shown in eqn (15) and (16), and the overall process for reactions with WCl_3, WCl_2 and WCl is shown in eqn (17) and (18).

$$HSiCl_3 + 2WCl_x = SiCl_4 + 2WCl_{x-1} + HCl \quad (15)$$

$$(CH_3)_2SiHCl + 2WCl_x = (CH_3)_2SiCl_2 + 2WCl_{x-1} + HCl \quad (16)$$

$$2HSiCl_3 + 2WCl_x = 2SiCl_4 + 2WCl_{x-1} + H_2 \quad (17)$$

$$2(CH_3)_2SiHCl + 2WCl_x = 2(CH_3)_2SiCl_2 + 2WCl_{x-1} + H_2 \quad (18)$$

3.4 Mechanism calculation of chlorination of $SiHCl_3$/$(CH_3)_2SiHCl$ with $MoCl_5$

3.4.1 Chain initiation reaction. The calculation process was the same as that in the previous section. By comparing the bond energies of Si–H bonds and Mo–Cl bonds in Tables 3 and 7, we can also divide the chain reaction into two reaction paths. In the processes involving $MoCl_5$ and $MoCl_4$ reactions with $SiHCl_3$ and $MoCl_5$, $MoCl_4$, $MoCl_3$ and MoCl reactions with $(CH_3)_2SiHCl$, Mo–Cl bond cleavage serves as the chain initiation reaction (eqn (19)). In the processes involving $MoCl_3$, $MoCl_2$, and MoCl reactions with $SiHCl_3$ and $MoCl_2$ reaction with $(CH_3)_2SiHCl$, chain initiation involves cleavage of the Si–H bonds (eqn (6) and (7)).

$$MoCl_x = MoCl_{x-1} + Cl\cdot \quad (19)$$

Table 7 Dissociation energies of Mo–Cl in $MoCl_x$

Compound	Parameter	DE/kJ mol^{-1}
$MoCl_5$	Mo–Cl	126.5
$MoCl_4$		281.5
$MoCl_3$		336.5
$MoCl_2$		347.2
MoCl		341.3

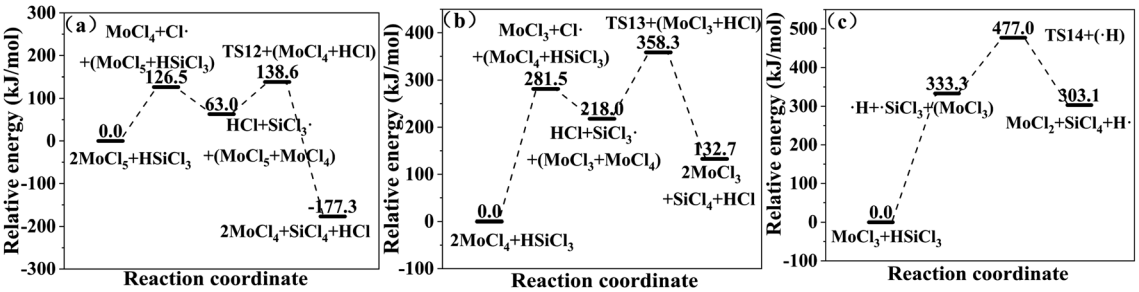

Fig. 9 (a–c) Relative energies for the reactions of $SiHCl_3$ with $MoCl_x$.

3.4.2 Chain propagation reaction. When the chain initiation reaction involves the release of Cl· from molybdenum chloride, chlorine atoms capture the hydrogen on the silicon to generate $SiCl_3^{\cdot}$ or $(CH_3)_2SiCl\cdot$ (eqn (8) and (10)). When the chain initiation reaction involves cleavage of Si–H bonds, $SiCl_3^{\cdot}$ or $(CH_3)_2SiCl\cdot$ is formed. The $SiCl_3^{\cdot}$ or $(CH_3)_2SiCl\cdot$ generated in the two reactions reacts with $MoCl_x$ (eqn (20) and (21)). The relative energies for the reactions of $SiHCl_3$ and $(CH_3)_2SiHCl$ with $MoCl_x$ are shown in Fig. 9 and 10. The structures of the transition states involved in these reactions are shown in Fig. 11.

$$MoCl_x + SiCl_3 = SiCl_4 + MoCl_{x-1} \quad (20)$$

$$MoCl_x + (CH_3)_2SiCl\cdot = (CH_3)_2SiCl_2 + MoCl_{x-1} \quad (21)$$

The main difference between the reactions of $MoCl_x$ with $SiHCl_3$ and $(CH_3)_2SiHCl$ lies in the energy barriers for the reactions of $\cdot SiCl_3$ and $\cdot(CH_3)_2SiCl$ with $MoCl_x$. Fig. 9 and 10 show the energy barriers and Gibbs free energy changes for $MoCl_x$ reactions with $SiCl_3^{\cdot}$ and $(CH_3)_2SiCl\cdot$, and these are summarized in Table 8. The energy barriers for the reactions of $MoCl_5$, $MoCl_4$, and $MoCl_3$ with $SiCl_3^{\cdot}$ are higher than those for the $(CH_3)_2SiCl\cdot$ reactions, and the differences are 75.6 kJ mol^{-1}, 72.7 kJ mol^{-1}, and 69.3 kJ mol^{-1}, respectively. The ΔG values for the $MoCl_5$, $MoCl_4$, $MoCl_3$, $MoCl_2$ and MoCl reactions with $SiCl_3^{\cdot}$ are all larger than the ΔG values for the corresponding $(CH_3)_2SiCl\cdot$ reactions. The above results reveal that $MoCl_x$ reacts more easily with $(CH_3)_2SiHCl$. In addition, the energy barrier difference between the reactions of $MoCl_5$ with $SiHCl_3$ and $(CH_3)_2SiHCl$ and the reactions of WCl_6 can be explained by the presence of only five Cl atoms in $MoCl_5$. WCl_6 is more conducive the chlorination of $(CH_3)_2SiHCl$ in $SiHCl_3$. Obviously, the calculated results are in good agreement with the experimental results.

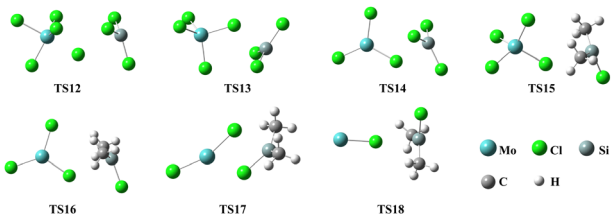

Fig. 11 Structures of transition states during the reactions of $SiHCl_3$/$(CH_3)_2SiHCl$ with $MoCl_5$.

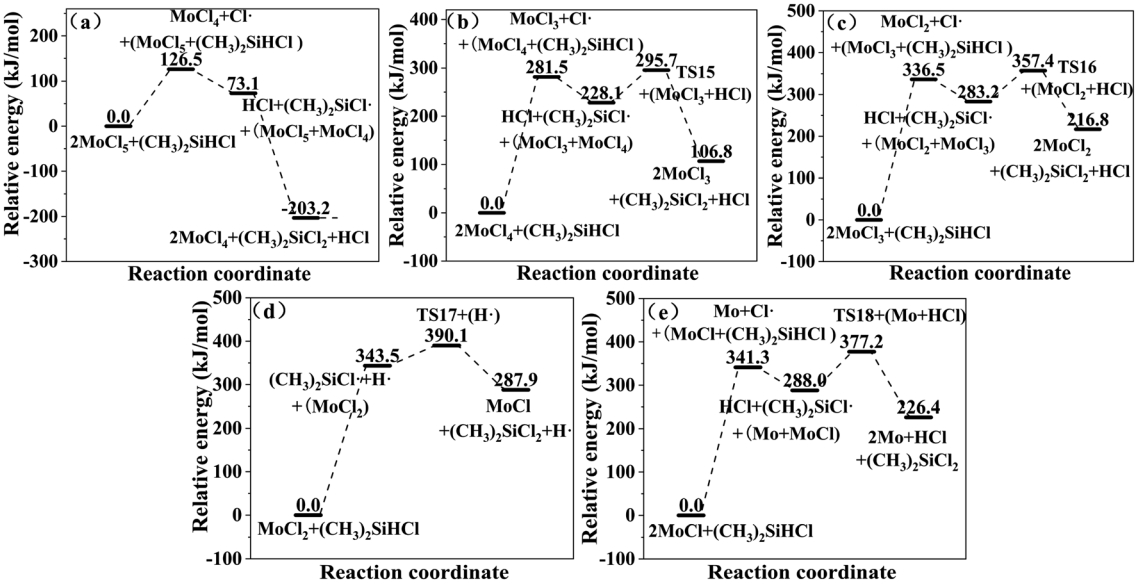

Fig. 10 (a–e) Relative energies for the reactions of $(CH_3)_2SiHCl$ with $MoCl_x$.

Table 8 Energy barriers and Gibbs free energy changes for $MoCl_x$ reactions with $SiCl_3^{\cdot}$ and $(CH_3)_2SiCl\cdot$

Reactant		EB (kJ mol^{-1})	ΔG (kJ mol^{-1})
$MoCl_5$	$\cdot SiCl_3$	75.6	−240.3
	$\cdot(CH_3)_2SiCl$	0	−276.3
$MoCl_4$	$\cdot SiCl_3$	140.3	−85.3
	$\cdot(CH_3)_2SiCl$	67.6	−121.3
$MoCl_3$	$\cdot SiCl_3$	143.6	−30.3
	$\cdot(CH_3)_2SiCl$	74.3	−66.4
$MoCl_2$	$\cdot SiCl_3$	—	−19.6
	$\cdot(CH_3)_2SiCl$	46.6	−55.6
MoCl	$\cdot SiCl_3$	—	−25.5
	$\cdot(CH_3)_2SiCl$	89.2	−61.6

3.4.3 Chain termination reaction. In the same way, in the $SiHCl_3$ reactions with $MoCl_5$ and $MoCl_4$ and the $(CH_3)_2SiHCl$ reactions with $MoCl_5$, $MoCl_4$, $MoCl_3$ and MoCl, chain termination occurs *via* a combination of $SiCl_3^{\cdot}$ and $(CH_3)_2SiCl\cdot$ reactions with $Cl\cdot$ (eqn (12) and (13)). In the processes for $SiHCl_3$ reactions with $MoCl_3$, $MoCl_2$ and MoCl and $(CH_3)_2SiHCl$ reaction with $MoCl_2$, chain termination occurs *via* the combination of two hydrogen atoms (eqn (14)).

Therefore, the overall equation for the reactions of $SiHCl_3$ with $MoCl_5$ and $MoCl_4$ is shown as eqn (22), and the overall equation for the reactions with $MoCl_3$, $MoCl_2$ and MoCl is shown as eqn (23). The overall equation of the reactions of $(CH_3)_2SiHCl$ with $MoCl_5$, $MoCl_4$, $MoCl_3$ and MoCl is shown as eqn (24), and the overall equation of the reaction with $MoCl_2$ is shown as eqn (25).

$$HSiCl_3 + 2MoCl_x = SiCl_4 + 2MoCl_{x-1} + HCl \quad (22)$$

$$2HSiCl_3 + 2MoCl_x = 2SiCl_4 + 2MoCl_{x-1} + H_2 \quad (23)$$

$$(CH_3)_2SiHCl + 2MoCl_x = (CH_3)_2SiCl_2 + 2MoCl_{x-1} + HCl \quad (24)$$

$$2(CH_3)_2SiHCl + 2MoCl_x = 2(CH_3)_2SiCl_2 + 2MoCl_{x-1} + H_2 \quad (25)$$

4. Conclusions

Chlorination reactions of $SiHCl_3$/$(CH_3)_2SiHCl$ were carried out with two metal chlorides (WCl_6 and $MoCl_5$) as the chlorine sources. The conversion rates for $(CH_3)_2SiHCl$ and $SiHCl_3$ both increased with increases in the reactant ratio, temperature and time. The conversions for the reactions of $(CH_3)_2SiHCl$ with WCl_6/$MoCl_5$ were much higher than those of $SiHCl_3$. Furthermore, the use of WCl_6 as the chlorine source showed higher conversion of the $(CH_3)_2SiHCl$ than $MoCl_5$. The optimum conditions for the reaction of WCl_6 with $(CH_3)_2SiHCl$ were as follows: a reaction pressure of 0.8 MPa, a reaction temperature of 60 °C, a reaction time of 60 min and $n(WCl_6) : n(SiHCl_3$ or $(CH_3)_2SiHCl) = 0.7$. The conversion rate for $(CH_3)_2SiHCl$ was 22.7 times that for $SiHCl_3$ in the reactions of $SiHCl_3$/$(CH_3)_2SiHCl$ with WCl_6.

The mechanisms for the reactions of $SiHCl_3$/$(CH_3)_2SiHCl$ with WCl_6/$MoCl_5$ were explored in detail with density functional theory calculations. The differences in the reactions of $SiHCl_3$ and $(CH_3)_2SiHCl$ with WCl_6 or $MoCl_5$ were found to lie in the energy barriers of the $SiCl_3^{\cdot}$ and $(CH_3)_2SiCl\cdot$ reactions with WCl_x/$MoCl_x$. The energy barriers for the reactions of WCl_x ($3 \leq x \leq 6$) with $SiCl_3^{\cdot}$ were higher than those for the $(CH_3)_2SiCl\cdot$ reaction. The same is true of $MoCl_x$ ($3 \leq x \leq 5$). On the whole, the energy barrier differences for WCl_6 reactions with $SiHCl_3$ and $(CH_3)_2SiHCl$ were higher than those for $MoCl_5$ reactions with $SiHCl_3$ and $(CH_3)_2SiHCl$. The experimental results were in good agreement with the calculation results. $(CH_3)_2SiHCl$ is converted to $(CH_3)_2SiCl_2$ in a chlorination reaction, which is conducive to the removal of carbonaceous impurities from $SiHCl_3$ by distillation in the improved Siemens method.

Conflicts of interest

There are no conflicts to declare.

Acknowledgements

This work was financially supported by the Major Science and Technology Project of Xinjiang Bingtuan (No. 2017AA007, 2020AA004) and the Major Science and Technology Project of Shihezi (No. 2020ZD02).

References

1 F. Chigondo, From Metallurgical-Grade to Solar-Grade Silicon: An Overview, *Silicon*, 2017, **10**, 789–798.
2 J. Gong, C. Li and M. R. Wasielewski, Advances in solar energy conversion, *Chem. Soc. Rev.*, 2019, **48**, 1862–1864.
3 N. Zhang, Q. Zheng, Y. Wang, D. Wang, W. Peng, J. Zhang, J. Zhang and J. Liu, Theoretical study on the reaction mechanism of Si_2Cl_6 and HCl catalyzed by amine catalysts, *New J. Chem.*, 2022, **46**, 17977–17984.
4 Q. Geng and G. Huang, Catalytic conversion of carbon-containing impurity methyldichlorosilane to purify raw material trichlorosilane of polysilicon production, *React. Chem. Eng.*, 2022, **2022**, 1544–1554.
5 S. Ranjan, S. Balaji, R. A. Panella and B. E. Ydstie, Silicon solar cell production, *Comput. Chem. Eng.*, 2011, **35**, 1439–1453.
6 G. Huang and M. Zhang, Reactive distillation purification method and device for removing carbon-containing impurities from chlorosilane, CN Pat., CN110980742A, 2020.
7 H. Wang, J. Chen, C. Hua and Y. Liu, Device and method for preparing high-purity trichlorosilane by adsorption of methyl chlorosilane impurities, CN Pat., CN109205627A, 2018.
8 Y. Wan, J. Xiao, D. Yan and J. Liu, Removal of methyldichlorosilane from trichlorosilane *via* photochemical chlorination, *Jingxi Huagong*, 2020, **37**, 201–206.
9 M. Zhang and G. Huang, Conversion reaction process of methyldichlorosilane in chlorosilane, *Jingxi Huagong*, 2020, **37**, 758–764.

10 M. Ishida, S. Hiroshi and H. Masyuki, Method for producing trichlorosilane, JP Pat., JP2014152093A, 2013.
11 H. Wang, J. Chen, C. Hua, Y. Liu and F. Li, Device and method for removing methyldichlorosilane from trichlorosilane by means of reactive distillation, WIPO Pat., WO2020103799A1, 2020.
12 K. Chulsky and R. Dobrovetsky, $B(C_6F_5)_3$-Catalyzed Selective Chlorination of Hydrosilanes, *Angew. Chem., Int. Ed.*, 2017, **56**, 4744–4748.
13 Y. Fu, Y. Jiang, H. Yin, L. Shen, Y. Feng and A. Wang, Catalytic chlorination of methylphenyldichlorosilane with gaseous chlorine to chlorinated methylphenyldichlorosilanes over Lewis acids, *J. Ind. Eng. Chem.*, 2014, **20**, 1022–1029.
14 H. Firouzabadi, N. Iranpoor and B. Karimi, Tungsten Hexachloride (WCl_6) in the Presence of Dimethylsulfoxide Promoted Facile and Efficient One-Pot Ring Expansion-Chlorination Reactions of 1,3-Dithiolanes and 1,3-Dithianes, *Synlett*, 1999, **1999**, 413–414.
15 B. Boualy, L. E. Firdoussi, M. A. Ali and A. Karim, Allylic chlorination of terpenic olefins using a combination of $MoCl_5$ and NaOCl, *J. Braz. Chem. Soc.*, 2011, **22**, 1259–1262.
16 A. A. Mekkaoui, M. Laayati, H. Orfi, L. El Firdoussi and S. El Houssame, Catalytic Allylic Chlorination of Natural Terpenic Olefins Using Supported and Nonsupported Lewis Acid Catalysts, *J. Chem.*, 2020, 2020.
17 S. Huo, H. Chen and W. Zuo, Selective Chlorination of Methane Photochemically Mediated by Ferric Chloride at Ambient Temperature, *Chin. J. Org. Chem.*, 2021, **41**, 1683–1690.
18 M. Frisch, G. Trucks, H. Schlegel, G. Scuseria, *et al.*, *Gaussian 16 Revision C. 01*, Gaussian, Inc., Wallingford CT, 2016.
19 C. Gonzalez and H. B. Schlegel, Reaction path following in mass-weighted internal coordinates, *J. Phys. Chem.*, 1990, **94**, 5523–5527.
20 R. V. G. Ewens and M. W. Lister, The structures of molybdenum pentachloride and tungsten hexachloride, *Trans. Faraday Soc.*, 1938, **34**, 1358–1362.
21 Y. Kawashima, The rotational spectrum of chlorodimethylsilane using Fourier transform microwave spectroscopy, *J. Mol. Struct.*, 2001, **563–564**, 227–230.
22 H. Takeo and C. Matsumura, The Microwave Spectra, Molecular Structures, and Quadrupole Coupling Constants of Methyltrichlorosilane and Trichlorosilane, *Bull. Chem. Soc. Jpn.*, 1977, **50**, 1633–1634.
23 J. D. DeSain, L. Valachovic, L. E. Jusinski and C. A. Taatjes, Reaction of chlorine atom with trichlorosilane from 296 to 473 K, *J. Chem. Phys.*, 2006, **125**, 224308.